



Structural and Optical Characteristics of Anatase and Rutile Titania Thin Films by Solvo-Thermal Doctor Blade Method

V. VETRIVEL^{1,*}, K. RAJENDRAN², T.S. SENTHIL³ and S. KARTHIKEYAN⁴

¹Department of Electronics & Communication Systems, Sri Krishna Arts & Science College, Coimbatore-641 008, India

²Department of Electronics, LRG Government Arts College for Women, Tirupur-641 604, India

³Department of Physics, Erode Sengunthar Engineering College, Erode-638 057, India

⁴Department of Chemistry, Chikkanna Government Arts College, Tirupur-641 602, India

*Corresponding author: E-mail: 2vetrivel@gmail.com

Received: 26 April 2016;

Accepted: 14 July 2016;

Published online: 29 October 2016;

AJC-18087

In present work, titania nanocrystal thin films were synthesized by using titanium(IV) isopropoxide as precursor and isopropyl alcohol as solvent. The precursor and solvent ratio were controlled to bring out the sol-gel. Triton X-100 was used to form titania paste and coated in FTO substrate by doctor blade method. The characteristic studies were carried out for the as-prepared sample, annealed at 450 °C and washed with HCl. The X-ray diffraction pattern revealed that anatase to rutile phase transformation for the as-prepared sample to the samples annealed at 450 °C and HCl washed. It also confirms the crystalline size of all the samples in nanoscale with average grain size of 5.71 nm and 18.76 nm. Scanning electron microscopy photograph confirms the presence of nanoparticles. The energy dispersive X-ray shows the prepared samples are titanium oxide without any impurity. The ultra violet-visual absorption study shows that the band gap of titania decrease with increase in annealing and HCl wash. Fourier transform infrared spectrum confirms the formation of titania.

Keywords: Titania, Nanoparticles, Sol-gel, Thin films, Dye-sensitized solar cell.

INTRODUCTION

Investigation of clean greener energy resources with efficient and low cost, dye-sensitized solar cell (DSSC) attracts much attention. Most of the dye-sensitized solar cell fabrication utilizes titania (TiO₂) coated TCO/FTO as working electrode. Titania is one among the important inorganic pigments used in the plastic and paint industry [1]. Moreover, the wide band gap energy of TiO₂, 3.2 eV is frequently studied in optic fields, especially as an excellent photo catalytic material applied in solar energy conversion and photo degradation [2,3]. Crystalline TiO₂ exists in three phases; brookite (orthorhombic), anatase (tetragonal with c/a\1) and rutile (tetragonal with c/a\1) [4]. Regan and Gratzel [5] have proposed wide band gap semiconductor metal organic complex dye based for dye-sensitized solar cells. Synthesis of TiO₂ nanoparticle thin film by sol-gel methods has proven to be a very useful tool for photo induced molecular reactions to take place on titanium dioxide surface. There are special variables that affect the photo induced reactions such as particle size, phase composition, incident light and preparation method [6]. There are several factors in deciding important properties of the titania for applications, such as particle size, crystalline and the morphology.

Titania (TiO₂) is an n-type semiconducting oxide [7]. The smaller the particle size of TiO₂, the larger the specific surface area. For the TiO₂ particles between 1 and 10 nm in size, the band-gap energy of TiO₂ depends on the particle size due to the quantum size effect: smaller the particle size, higher is the band-gap energy of TiO₂ [8].

In last few years, nanocrystalline TiO₂ thin films have received much attention for solar energy applications [9]. Due to the high demand of titania in different applications, simple and low cost techniques are required for titania preparation. Although TiO₂ with different shape has been synthesized by different methods, the formation mechanisms of titania with different shape remains a challenge in this field [10]. Many methods are available for the preparation of titania. But sol-gel method is simple and easiest method to procure titania nanoparticles. In this paper, we reported the effect of annealing and washing in preparation of titania nanoparticle thin film.

EXPERIMENTAL

Titania (TiO₂) nanocrystalline thin films were prepared by solvo-thermal and doctor blade method. TiO₂ nanocrystals were derived *via* non-aqueous sol-gel precipitation of titanium(IV)

isopropoxide $\text{Ti}[\text{OCH}(\text{CH}_3)_2]_4$ (Aldrich, 99.9 %), followed by hydrothermal treatment and calcinations. Titanium(IV) isopropoxide was used as titania precursor, isopropanol was used as solvent. The sol was prepared by mixing 1.1 mL of titanium(IV) isopropoxide (TIP) with 15 mL of isopropanol at room temperature and stirred for 1 h. Later titanium(IV) isopropoxide is added dropwise and stirred vigorously and obtained a homogeneous mixture of TiO_2 sol. The colour of the prepared sol was in moonstone yellow having $\text{pH} = 5.8$. The mixed solution was then transferred into a 100 mL Teflon autoclave without stirrer, sealed with a stainless steel lid and aged at 120 °C for 24 h and then aged at an elevated hydrothermal temperature of 150 °C for desired period of 48 h for the nucleation and growth of titania particles. The obtained white gel products were centrifuged and washed at 4500 rpm for 5 min. A part of titania gel was washed with deionized water and another part of titania gel was washed with 0.1 M of HCl. Thus obtained nanocrystalline gel was dried in hot air oven for 100 °C and crushed to powder. Titania powder was added dropwise with Triton X-100 to form a titania paste. Then the paste was coated in FTO glass slides using doctor blade method. Prior to coating of thin film, the conductive side of FTO was identified using multimeter and ultrasonically cleaned with ethanol and deionized water. Titania paste was applied on the conductive side of the FTO plate for the formation of titania thin film using doctor blade method. The deionized water washed, powder coated FTO dried in hot air oven was named as as-prepared sample and the same annealed at 450 °C as Annealed sample, whereas HCl washed titania nano powder coated FTO annealed at 450 °C was named as HCl washed sample.

RESULTS AND DISCUSSION

X-ray diffraction studies: Fig. 1 represents the X-ray diffraction (XRD) pattern of the synthesized titania thin films as a function of three different preparation methods. The d-spacing values of as-prepared, 450 °C annealed and HCl washed samples corresponding to the diffraction peaks are compared with the standard data (JCPDS, powder diffraction file No. 84-1286 and 21-1276) and found to be in good agreement with the anatase phase and rutile phase of titania [11]. The sharp peaks of the XRD pattern indicate that the synthesized titania particles are well crystalline in nature [12]. The lattice constants have been calculated as $a = 3.80126$, $c = 9.502$ for titania as-prepared and $a = 4.611736$, $c = 2.944808$ for titania annealed at 450 °C and $a = 4.627886$, $c = 2.974031$ for HCl washed titania. Which are agreed well with standard JCPDS data. In addition, the broadening of XRD peaks which

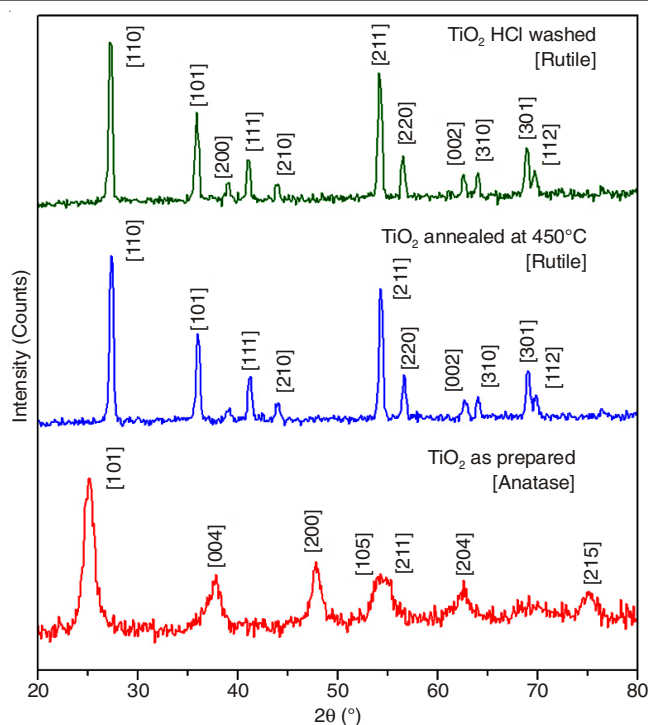


Fig. 1. X-ray diffraction patterns of titania thinfilms for three different preparation methods (as-prepared, annealed at 450 °C and HCl washed)

in turn to leads particles in small size [13]. From the XRD data, the broadening of the XRD peaks gradually decreases with different preparation method, which has been shown in Table-1. The average crystallite sizes were calculated from Debye-Scherrer formula:

$$D_{\text{avg}} = k\lambda/\beta\cos\theta$$

where, k denotes the Scherrer constant ($k = 0.94$), $\lambda = 1.5406$ Å is the wavelength of the incident radiation, β is the FWHM height of the diffraction peak at angle θ [14]. The average crystallite sizes have been calculated as 5.71, 6.43 and 7.25 nm for the as-prepared sample of titania, 15.98, 17.04, 18.86 nm for the annealed sample and 17.63, 17.75 and 18.67 nm for the HCl washed sample of titania. The specific surface area of the samples has been calculated as [15]:

$$S = 6 \times 10^3/\rho D \text{ m}^2/\text{g}$$

where, S is the specific surface area (m^2/g), ρ is the density of TiO_2 (3.89 g/cm^3 for anatase [16] and 4.23 g/cm^3 for rutile [17]) and D is the average crystallite size. The specific surface area is increased as the particle size becomes small (Table-1). It is shown that the increase in XRD peak width, decreases

TABLE-1
AVERAGE CRYSTALLINE SIZE (D) AND SPECIFIC SURFACE AREA (SSA) FOR TITANIA THINFILMS

Sample ID	k	λ (nm)	2 θ	θ	cos θ	β (radians)	D (nm)	SSA (m^2/g)
As-prepared	0.94	0.15406	37.6437	18.8218	0.9465	0.023984	5.71	269.81
As-prepared	0.94	0.15406	25.0852	12.5426	0.9761	0.021825	6.43	239.87
As-prepared	0.94	0.15406	47.8181	23.9090	0.9141	0.018886	7.25	212.45
Annealed	0.94	0.15406	27.3267	13.6633	0.9717	0.008827	15.98	88.73
Annealed	0.94	0.15406	35.9771	17.9885	0.9511	0.008042	17.04	83.20
Annealed	0.94	0.15406	54.2562	27.1281	0.8899	0.007269	18.86	75.20
HCl washed	0.94	0.15406	27.2295	13.6147	0.9719	0.007998	17.63	80.41
HCl washed	0.94	0.15406	35.8631	17.9315	0.9514	0.008119	17.75	79.91
HCl washed	0.94	0.15406	54.1623	27.0811	0.8903	0.008244	18.67	75.93

average crystallite size and increases specific surface area. The increased specific surface area leads to more dye absorption in dye sensitized solar cells and increased current density [18].

Energy dispersive X-ray analysis: The composition and purity of the prepared sample has been studied by energy dispersive X-ray analysis (EDX). Figs. 2a-2c shows typical composition of materials found. The EDX spectrum shown in Figs. 2a-2c exhibits the presence of only oxide and titania, suggesting the particles are indeed made up of O and Ti. The inset shows the ratio of O and Ti ion concentration. The spectrum is devoid of any other metal ion which indicates the purity of the prepared samples.

Fig. 2a shows high peak for oxide than titania, this is due to the fact, prepared sample possess more oxygen contents. Whereas the annealed sample of Figs. 2b-2c shows the oxide content decreased, when compared to as-prepared sample. This may be attributed to the reduction of oxygen due to annealing. In same context the effect of HCl washed sample does not make much deviation with deionized water washed sample. The EDX spectra analysis shows that all the three samples have titania and oxide content with no traces of other materials. The EDX analysis shows that the prepared TiO₂ samples are in pure form without any impurities.

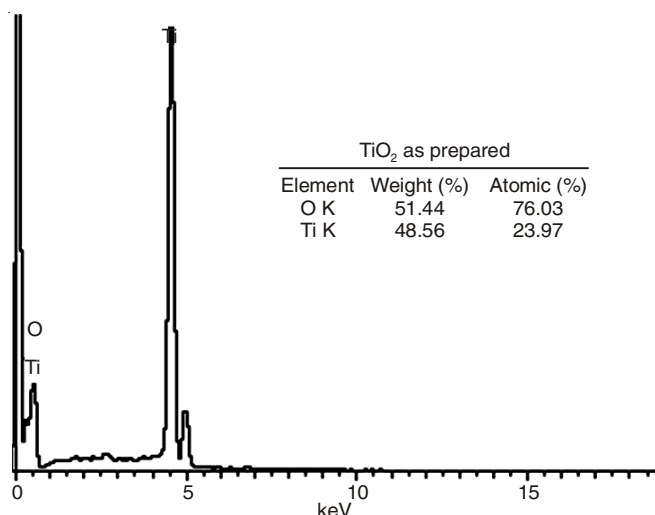


Fig. 2(a): EDAX spectrum of titania as-prepared

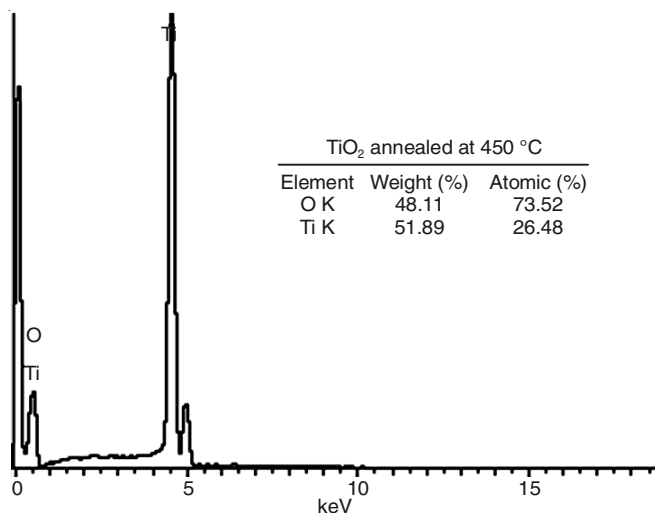


Fig. 2(b): EDAX spectrum of titania annealed at 450 °C

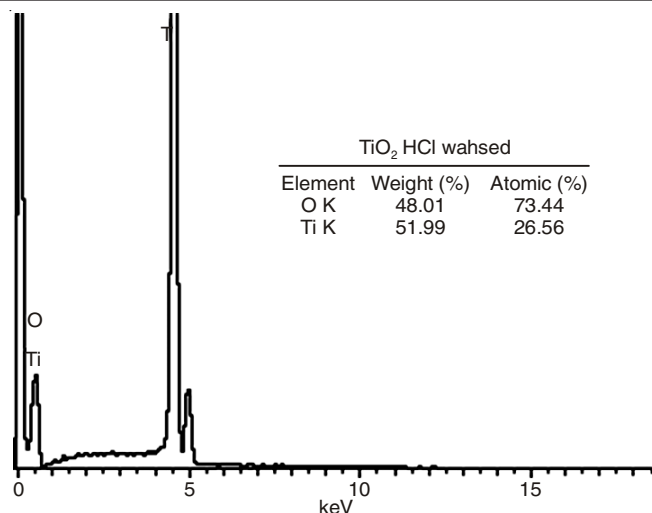


Fig. 2(c): EDAX spectrum of titania HCl washed

UV-visible spectroscopy: UV-visible spectrophotometer is basically known as ultraviolet-visible spectroscopy. It measures the intensity of light passing through a sample (*I*) and compares it to the intensity of light before it passes through the sample (*I*₀). The ratio *I*/*I*₀ is called the transmittance and is usually expressed as a percentage (%T). The absorbance (*A*), is based on the transmittance $A = -\log(\%T/100\%)$. Fig. 3 shows the absorption spectrum of titania at different preparation methods, the cutoff wavelength is observed at 339.09 nm for as-prepared sample, 342.86 nm for annealed sample and 348.15 nm for HCl washed sample. The band gap energy of titania thin films has been calculated as:

$$\text{Band gap energy (Eg)} = h \cdot C / l$$

where, *h* = Planks constant, *C* = Velocity of light and *l* = Cut off wavelength. Tauc method [19] is followed to find the band gap from the absorbance graph. From the Fig. 3, the energy band gap of as-prepared titania is found to be 3.66 eV at 339.09 nm wavelength, annealed titania is 3.62 eV at 342.86 nm wavelength and HCl washed titania is 3.57 eV at 348.15 nm wavelength. The observed band gap wavelength shows red shift towards preparation methods. It is noticed annealing and HCl wash helped in increased size of nanoparticles and in turn

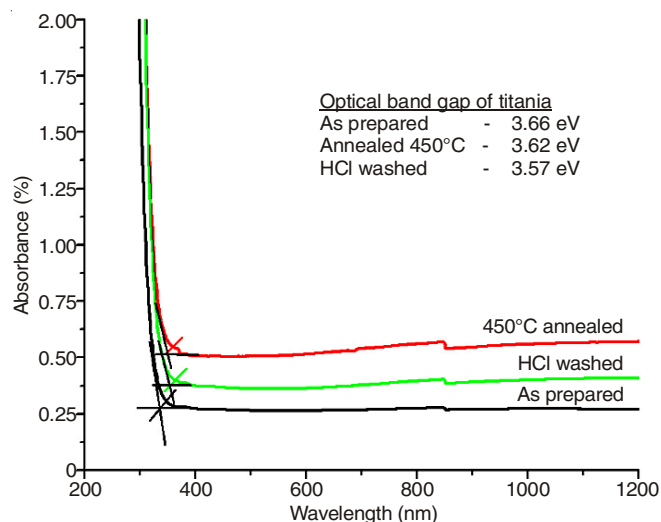


Fig. 3. UV visible spectrum of titania, with band gap

increased nano size decreases the band gap of the material [20]. Band gap increment of anatase TiO_2 would be larger than that of rutile TiO_2 [20], wide band gap oxides is well suited for light harvesting in dye sensitized solar cells [21].

Fourier transform infrared spectroscopy: It is absorbed that Fourier transform infrared spectroscopy (FTIR) spectra for as-prepared titania differs from annealed sample and HCl washed sample titania. The annealed and HCl washed FTIR spectra coordinates with each other. The FTIR spectra of as-prepared sample, the strong peaks absorbed are 3988.89, 3888.49, 3402.43, 2924.09, 2854.65, 2345.44, 1627.92, 1458.18, 516.92. The FTIR spectra of annealed titania, the strong peaks absorbed are 3927.07, 3865.35, 3749.52, 3425.58, 2924.09, 2854.65, 1627.92, 1442.75, 486.06. The strong peaks of HCl washed titania are observed at 3749.62, 3433.29, 2924.09, 2854.65, 1627.92, 1442.75, 524.65 cm^{-1} .

The peaks observed in between 3900 to 2854 cm^{-1} can be assigned to stretching vibrations of hydroxyl groups. The presence of hydroxyl groups exhibits the coordination vacancies in the presence of water. They are attributed to the atmospheric water/ethanol used during the synthesis process. The bending vibration band of the $-\text{OH}$ group was observed at 1627 cm^{-1} . It is attributed to deformation vibrations of molecular water. The TiO_2 particle annealed at high temperature are in favour of water adsorption onto the surface. These are visible since the FTIR is done at room temperature in ambient conditions [22]. In TiO_2 , broad band around 3750 cm^{-1} corresponds to Ti-O-Ti and O-H stretching frequencies [23]. In the spectrum of pure TiO_2 , the peaks at 524.65 cm^{-1} show stretching vibration of Ti-O and peaks at 1442.75 cm^{-1} shows stretching vibrations of Ti-O-Ti. Peaks at 3402.43, 3425.58, 3433.29 cm^{-1} indicate the presence of amines [6]. The rutile samples of TiO_2 are characterized by a broad strong band with transmittance minima at 524.65 cm^{-1} assigned to vibrations of Ti-O and Ti-O-Ti framework bonds [24,25].

Scanning electron microscopy: The morphology of the titania thin film have been examined by scanning electron microscopy imaging at different magnifications. The SEM images reveal the perfectly solid shapes of titania particles. Fig. 4(a) shows the growth of titania as-prepared sample with plain surface and the particle size estimated from the SEM images is 20-40 nm. Fig. 4(b) shows the SEM image of titania annealed at 450 °C that is nano sized distributed surface and approximated particle size of 40-54 nm. Fig. 4(c) shows the SEM image of HCl washed titania, that is nano sized scatterly distributed surface, irregular, hetrogenous and approximated particle size of 40-154 nm. By different preparation methods with effect to temperature and wash, the nucleation rate of the particles decreases rapidly.

Conclusion

Titania thin films were successfully prepared in three different methods using non-aqueous solvo-thermal. Phase change of anatase to rutile of titania is achieved at lowest possible temperature. The average crystalline size of anatase phase found to be 6.46 nm and rutile phase is 17.29 nm and 18.01 nm for 450 °C annealed sample and HCl washed sample, respectively. Lattice parameters confirms the titania in tetragonal shape. Average specific surface area of anatase phase titania is

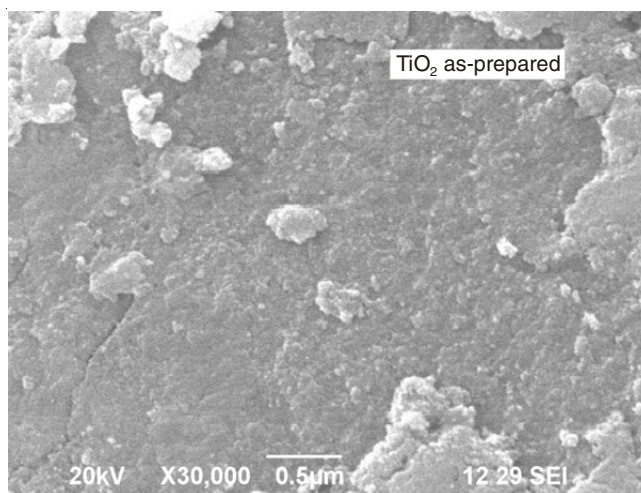


Fig. 4(a). SEM image of titania as-prepared

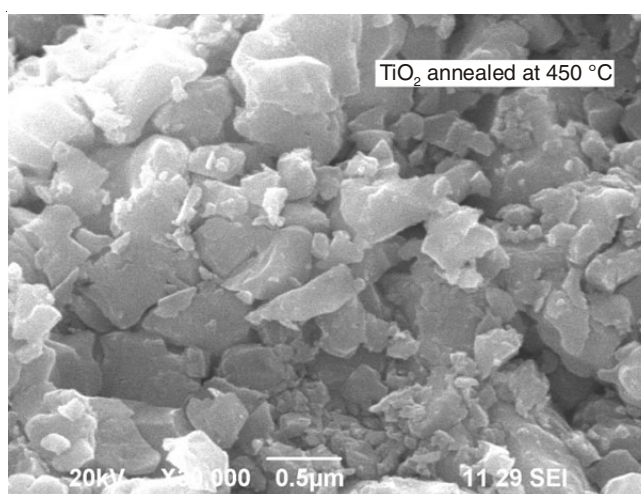


Fig. 4(b). SEM image of titania annealed at 450 °C

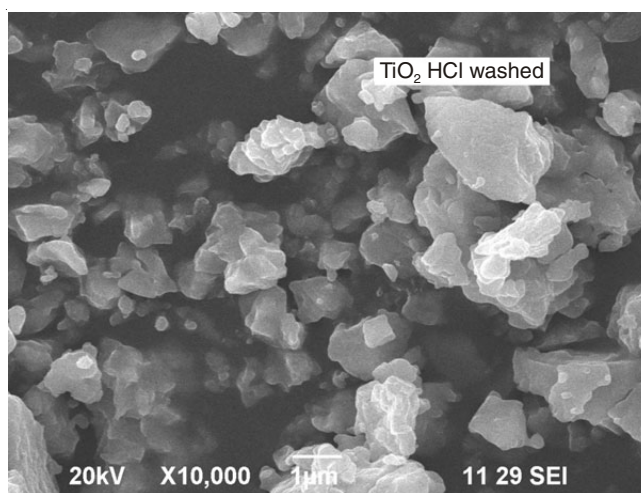


Fig. 4(c). SEM image of titania HCl washed

361.065 m^2/g and rutile phase titania is 82.37 m^2/g and 78.75 m^2/g . In both cases anatase titania holds good nanocrystalline and large specific surface area for more dye absorption which leads to higher current density for dye-sensitized solar cell applications. Good stoichiometric ratio in EDX spectrum, clearly defines there is no impurities found in the prepared

samples. The optical band gap energy of as-prepared (anatase) sample is 3.66 eV, annealed (rutile) sample is 3.62 eV and HCl washed (rutile) sample is 3.57 eV, which terms to be higher than the bulk. As higher band gap oxide is suitable for dye-sensitized solar cell, hence anatase titania is best preference for dye-sensitized solar cell applications. FTIR confirms pure titania spectrum in Ti-O-Ti and O-H stretching frequencies and vibrations of Ti-O and Ti-O-Ti framework bonds. SEM indicates the formation of nano crystals in both phases of titania. The optimum titania phase for dye-sensitized solar cell is found to be anatase phase rather than rutile phase of titania.

REFERENCES

1. D. Sridhar and N. Sriharan, *J. NanoSci. NanoTechnol.*, **2**, 94 (2014).
2. F. Bosc, A. Ayrat, P.-A. Albouy and C. Guizard, *Chem. Mater.*, **15**, 2463 (2003).
3. H. Hänsel, H. Zettl, G. Krausch, R. Kisselev, M. Thelakkat and H.-W. Schmidt, *Adv. Mater.*, **15**, 2056 (2003).
4. V. Vetrivel and K. Rajendran, *Int. J. Sci. Res.*, **3**, 57 (2014).
5. B. O'Regan and M. Gratzel, *Nature*, **353**, 737 (1991).
6. V. Vetrivel, K. Rajendran and V. Kalaiselvi, *Int. J. ChemTech. Res.*, **7**, 1090 (2015).
7. N. Sriharan and M. Gunabal, UGC sponsored National Level Conference on Advanced Materials (NCAM-2015); ISBN 978-93-84743-38-3 (2015).
8. N. Gokilamani, N. Muthukumarasamy and M. Thambidurai, *Adv. Mater. Res.*, **678**, 108 (2013).
9. T.S. Senthil, N. Muthukumarasamy, D. Velauthapillai, M. Thambidurai, S. Agilan and R. Balasundaraprabhu, *Renew. Energy*, **36**, 2484 (2011).
10. T.S. Senthil, N. Muthukumarasamy, M. Thambidurai, R. Balasundaraprabhu and S. Agilan, *J. Sol-Gel Sci. Technol.*, **58**, 296 (2011).
11. V. Vetrivel, K. Rajendran, T. S. Senthil and P. Anbarasu, *J. Environ. Nanotechnol.*, **5**, 08 (2016).
12. Q. Chen, W. Zhou, G.H. Du and L.-M. Peng, *Adv. Mater.*, **14**, 1208 (2002).
13. A. Chemseddine and T. Moritz, *Eur. J. Inorg. Chem.*, 235 (1999).
14. N. Gokilamani, N. Muthukumarasamy, M. Thambidurai, A. Ranjitha and D. Velauthapillai, *J. Sol-Gel Sci. Technol.*, **66**, 212 (2013).
15. A. Kolary-Zurowska, A. Zurowski, R. Marassi and P.J. Kulesza, *ECS Trans.*, **28**, 89 (2010).
16. L. Kavan, M. Grätzel, J. Rathouský and A. Zukal, *J. Electrochem. Soc.*, **143**, 394 (1996).
17. D.G. Isaak, J.D. Carnes, O.L. Anderson, H. Cynn and E. Hake, *Phys. Chem. Miner.*, **26**, 31 (1998).
18. B. Tan and Y. Wu, *J. Phys. Chem. B*, **110**, 15932 (2006).
19. T.S. Senthil, N. Muthukumarasamy and M. Kang, *Opt. Lett.*, **39**, 1865 (2014).
20. H.-S. Lee, C.-S. Woo, B.-K. Youn, S.-Y. Kim, S.-T. Oh, Y.-E. Sung and H.-I. Lee, *Top. Catal.*, **35**, 255 (2005).
21. A.J. Nozik, *Physica E*, **14**, 115 (2002).
22. Y. Li, X. Sun, H. Li, S. Wang and Y. Wei, *Powder Technol.*, **194**, 149 (2009).
23. R. Ganesan and A. Gedanken, *Nanotechnology*, **19**, 435709 (2008).
24. K. Chhor, J.F. Bocquet and C. Pommier, *Mater. Chem. Phys.*, **32**, 249 (1992).
25. A. Larbot, I. Laaziz, J. Marignan and J.F. Quinson, *J. Non-Cryst. Solids*, **147-148**, 157 (1992).